



DISPLACEMENT-BASED SEISMIC DESIGN OF NON-STRUCTURAL BUILDING ELEMENTS

A. Filiatrault⁽¹⁾, R.J. Merino⁽²⁾, D. Perrone⁽³⁾, G.M. Calvi⁽⁴⁾

⁽¹⁾ Professor, University School for Advanced Studies IUSS Pavia, Italy and State University of New York at Buffalo, USA,

⁽²⁾ PhD student, University School for Advanced Studies IUSS Pavia, Italy, roberto.javier.merinovela@iusspavia.it

⁽³⁾ Research Fellow, University School for Advanced Studies IUSS Pavia, Italy, daniele.perrone@iusspavia.it

⁽⁴⁾ Professor, University School for Advanced Studies IUSS Pavia, Italy, gm.calvi@iusspavia.it

Abstract

Damage observed during past earthquakes, as well as recent loss estimation studies, have demonstrated the importance of the seismic design of non-structural elements. In a performance-based seismic design framework, the achievement of adequate performance objectives is not only related to the performance of the structure but also to the response of non-structural elements. Because of lack of information on the seismic performance of non-structural elements, current seismic design provisions are either empirical in nature or based on judgement and lack clear definitions of performance objectives under specific seismic hazard levels. Current seismic design provisions are generally based on an empirical force-based seismic design approach. To address these shortcomings, this paper proposes a direct displacement-based methodology for the seismic design of non-structural elements in buildings. The proposed displacement-based design procedure applies mainly to acceleration-sensitive non-structural elements suspended or anchored at a single location (floor) in the supporting structure and for which damage is the result of excessive relative displacements. Examples of such acceleration-sensitive non-structural elements are suspended building utility systems, such as piping systems and cable trays, and anchored, free standing and vibration isolated building utility systems or contents. The design of the seismic restraints for a horizontal mechanical piping system suspended from the top floor of a generic case-study six-story steel moment-resisting frame building assumed to be located in high seismic site in the Western United States (US) was performed both according to the proposed direct displacement-based procedure and to the force-based design procedure of the ASCE 7-16 Standard in the US. Both design alternatives were evaluated through nonlinear time-history dynamic analyses in order to evaluate the effectiveness of the direct displacement-based design methodology as well as the influence of the design assumptions needed to perform the force-based design procedure.

Keywords: Non-structural elements, nonstructural components, direct displacement-based design, pipes, suspended piping restraint installations.



1. Introduction

The performance-based seismic design of structures has advanced considerably during the last two decades. However, its application to the design of non-structural elements remains largely unexplored. Recent loss estimation studies, as well as the damage observed during recent earthquakes in densely built areas, repeatedly demonstrated the importance of non-structural elements and their vulnerability even under low to moderate earthquakes [1-4]. In comparison to structural elements and systems, there is much less information and specific guidance available on the seismic design of non-structural building elements for multiple performance objectives [5-7]. As a consequence, the prescriptive design information currently available is based largely on engineering judgement rather than on scientific experimental and analytical results.

Current seismic provisions distinguish between acceleration-sensitive and displacement-sensitive non-structural elements. For acceleration-sensitive non-structural elements, equivalent static design forces are specified while in the case of displacement-sensitive non-structural elements, limits are imposed on the inter-storey drifts of the supporting structure [6, 7]. Non-structural building elements would benefit greatly from rational performance-based seismic design procedures. To this aim, a direct displacement-based seismic design procedure has been recently developed by Filiatrault *et al.* [8]. This methodology, which is inspired from the existing displacement-based seismic design procedure for structural systems [14], applies to acceleration-sensitive non-structural elements suspended or anchored at a single location (floor) in the supporting structure and for which the damage is the results of excessive relative displacements.

This paper compares the traditional force-based seismic design approach, included in Chapter 13 of the ASCE 7-16 Standard [7] in the United States (US), with the direct displacement-based procedure recently proposed by Filiatrault *et al.* [8]. The comparison was conducted by performing the design of the seismic restraints for a suspended horizontal mechanical piping system. The effectiveness of the two seismic design approaches was appraised through nonlinear time history analyses.

2. ASCE 7-16 Force-Based Seismic Design of Non-Structural Elements

The seismic provisions of current European and North American design standards require that acceleration-sensitive non-structural elements and/or its connections to the supporting structure be designed for equivalent static design forces in the horizontal and/or vertical directions applied at the element's centre of mass. The ASCE 7-16 Standard [7] in the US prescribes the following horizontal and vertical equivalent static design forces, F_{ph} and F_{pv} :

$$F_{ph} = \frac{0.4a_p S_{DS}}{\left(\frac{R_p}{I_p}\right)} \left(1 + 2\frac{z}{h}\right) W_p \quad (1)$$

$$F_{pv} = \pm 0.2 S_{DS} W_p \quad (2)$$

where a_p is the element amplification factor taking values of 1 for rigid elements (natural period T_p less equal than 0.06 s) or 2.5 for flexible elements ($T_p > 0.06$ s), S_{DS} is the design spectral acceleration at short (0.2 s) period, R_p is the element response modification factor taking values from 1 to 12 depending on the type of non-structural element, I_p is the element importance factor taking values of 1 for ordinary elements or 1.5 for critical elements, z is the elevation of the centre of mass of the non-structural element relative to the base elevation of the supporting structure, h is the average roof height of the supporting structure relative to its base elevation and W_p is the operating weight of the element. The horizontal and vertical equivalent static design forces given by Eqs. (1) and (2) are generally used to design the non-structural element and its attachments to the supporting structure.

Although the simple force-based design approach for non-structural elements has been used extensively and remains the cornerstone of seismic design requirements included in current editions of building codes, it includes several major shortcomings. These shortcomings, expressed specifically in terms of the ASCE 7-16 force-based design procedure, are itemized below.



1. The element's amplification factor, a_p , in Eq. (1), representing the expected dynamic amplification of the peak floor acceleration at the centre of mass of the non-structural element, does not consider the damping characteristics of the element and neglects non-linear response of both the supporting structure and the non-structural element.
2. The empirical linear amplification of the peak floor acceleration with respect to the peak ground acceleration ($1+2z/H$ term in Eq. [1]) assumes first mode response of the supporting structure. The establishment of reasonable estimates for the peak floor-acceleration-response profile along the height of buildings has been the subject of numerous studies and is still controversial due particularly to higher mode effects in buildings [9-13].
3. The force response modification factor assigned to the non-structural element, R_p , in Eq. (1) is difficult to justify since it is based primarily on judgment. Particularly, the lack of information on the lateral load-deformation response of many non-structural element typologies makes the use of current non-structural force reduction factors misleading. Also, R_p is associated with the global displacement ductility capacity of the non-structural element. This displacement ductility is based on the ratio of a performance limit displacement to a first-yield displacement. No appropriate definitions of yield and performance limit displacements have been formulated for non-structural elements.
4. Deformation limit states of non-structural elements are not directly addressed by the force-based design procedure. Limiting deformations is paramount for non-structural elements, as stated qualitatively in building codes, since a large portion of the non-structural damage from recent earthquakes has been associated with excessive lateral displacements of the non-structural elements relative to the supporting structure.

These limitations of the forced-based seismic design procedure do not allow for a proper assessment of the seismic safety of non-structural building elements considering the various limit states that these elements may have to confront during their service lives. A performance-based seismic design approach for non-structural elements should consider relative displacements to the supporting structure as the central focus of the design process. For many acceleration-sensitive non-structural elements, this can be achieved by using a direct displacement-based seismic design procedure.

3. Direct Displacement-Based Seismic Design of Non-Structural Elements

Recently Filiatrault *et al.* [8] adapted the existing direct-displacement based design (DDBD) procedure originally developed for structural systems [14] to the seismic design of acceleration-sensitive non-structural elements attached to a single point (floor) on the supporting structure, and for which the damage occurs due to excessive relative displacements. Non-structural element typologies for which the proposed DDBD procedure applies include piping systems (including sprinklers), cable trays, suspended ceilings, cantilevered parapets, raised access floors, anchored shelves and out-of-plane partitions, cladding and glazing. Figure 1 presents a flow chart illustrating the various steps of the DDBD process for non-structural elements. These steps are discussed in this section along with a description of the information required to apply the DDBD methodology. More details on the procedure are provided in Filiatrault *et al.* [8].

The DDBD procedure starts with the definition of the target displacement, $\Delta_{t,p}$, or ductility, $\mu_{t,p}$, that the non-structural element should not exceed under a given seismic hazard level. This target displacement is associated with the acceptable peak deformation of the non-structural element relative to its attachment point on the supporting structure. The seismic hazard associated with the target displacement must then be defined in terms of a design floor relative displacement response spectrum. Several performance objectives could be considered simultaneously [4]. Significant efforts have been made in recent years to develop simplified but accurate means of estimating design absolute acceleration floor response spectra [15-19]. Once a design absolute acceleration floor response spectrum is constructed, the floor relative displacement response spectrum can be easily obtained by using the usual pseudo-spectral relationship [20]. In the design example described later, the procedure developed by Merino *et al.* [19] to construct consistent absolute acceleration and relative displacement floor response spectra was used.

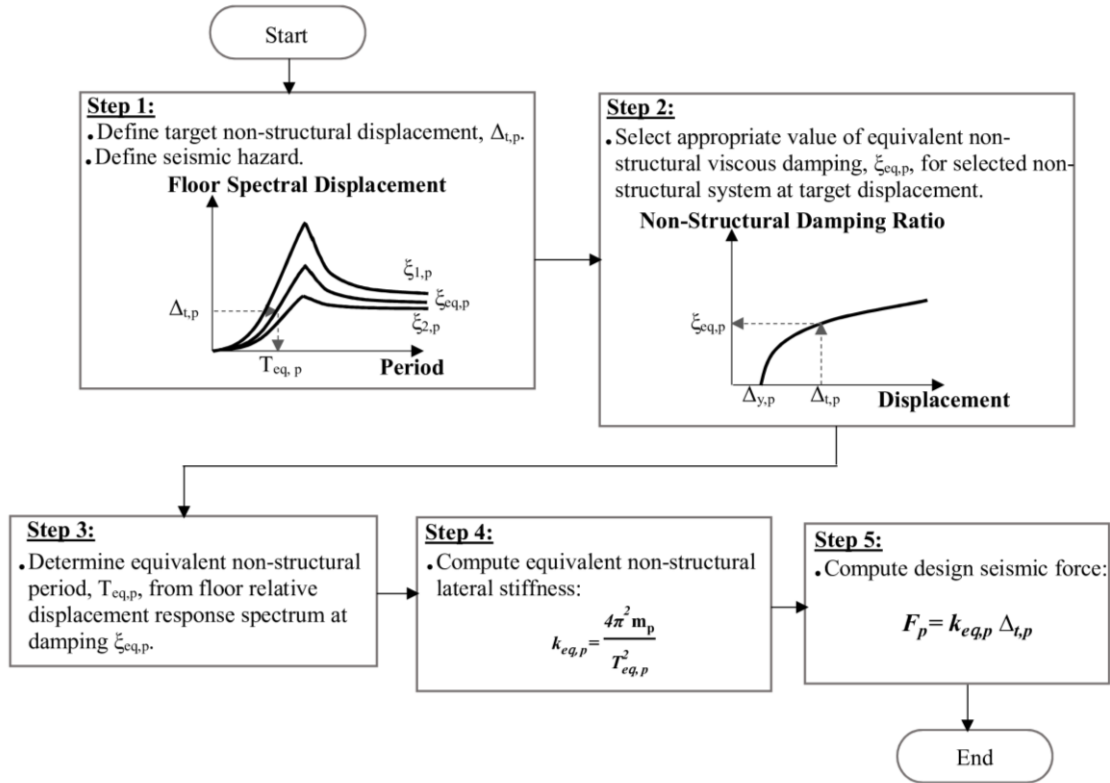


Fig. 1 – Flowchart of DDBD of non-structural elements, after [8].

The second step of the DDBD procedure consists in estimating the energy dissipation characteristics of the non-structural element at the target non-structural displacement, $\Delta_{t,p}$, (or ductility $\mu_{t,p}$). This quantity is represented by an equivalent viscous damping ratio, $\xi_{eq,p}$. For this purpose, a non-structural damping database, in the form of a $\xi_{eq,p} - \Delta_{t,p}$ (or $\xi_{eq,p} - \mu_{t,p}$) relationship, must be developed from cyclic testing data on the non-structural element typology under consideration. Once this non-structural damping database has been established, $\xi_{eq,p}$ can be established using the energy-based equivalent viscous damping approach originally proposed by Jacobsen [21].

$$\xi_{eq,p} = \frac{E_{D,\Delta_{t,p}}}{2\pi k_{eq,p} \Delta_{t,p}^2} + \xi_{i,p} \quad (3)$$

where $E_{D,\Delta_{t,p}}$ is the energy dissipated per cycle by the non-structural element at the target displacement, $k_{eq,p}$ is the equivalent lateral stiffness of the non-structural element at the target displacement. A nominal inherent damping ratio, $\xi_{i,p}$, can also be considered to account for the energy dissipation not associated with the hysteretic response of the non-structural element.

Knowing the target displacement, $\Delta_{t,p}$, and the equivalent viscous damping ratio, $\xi_{eq,p}$, of the non-structural element at that target displacement, the equivalent (secant) period of the non-structural element, $T_{eq,p}$, can be obtained in Step 3 directly from the design floor relative displacement response spectrum derived in Step 1. The non-structural equivalent lateral stiffness, $k_{eq,p}$, can be obtained in Step 4 as follows:

$$k_{eq,p} = \frac{4\pi^2 W_p}{g T_{eq,p}^2} \quad (4)$$

Finally, in Step 5, the resulting design force, F_p , on the non-structural element can be computed by:

$$F_p = k_{eq,p} \Delta_{t,p} \quad (5)$$



This design force can then be applied at the centre of mass of the non-structural element and used to design the specific bracing/anchorage components supporting the non-structural element and/or the non-structural element itself. Note that no iteration on $k_{eq,p}$ is required since the equivalent period of the non-structural element, $T_{eq,p}$, is obtained directly from the floor response spectrum at the proper damping level and that the operating weight, W_p , and damping ratio, $\xi_{eq,p}$, of the element are known at the design non-structural displacement $\Delta_{i,p}$.

4. Design Example: Suspended Piping Seismic Restraint Installations

To illustrate the applications of the force-based design approach included in the ASCE 7-16 [7] and of the proposed DDBD procedure previously described, the design of the seismic restraints for a horizontal mechanical piping system is performed. The mechanical piping system is suspended from the top floor of a generic case-study six-storey steel moment-resisting frame building located in a high seismicity site with a Seismic Design Category D in the US. Descriptions of the supporting structure, the mechanical piping system, and the results of the design calculations are provided in this section. The performance of both design approaches are appraised by nonlinear dynamic time-history analyses in the next section.

4.1 Case-study building and site characteristics

The case study building consists of a six-storey steel building, rectangular in shape and braced in the North-South direction by two exterior moment-resisting frames. The height of the ground storey is equal to 5.48 m, while the heights of the upper storeys are 3.8 m. Design gravity loads include the roof dead load (3.8 kPa), the floor dead load (4.5 kPa), the roof live load (1.0kPa), the floor live load (3.8 kPa), and the weight of the exterior cladding (1.7 kPa). The steel grade is assumed to be A36 (nominal $F_y = 290$ MPa) for all members. The details of the beams and columns are shown in Fig. 2. The building is assumed to be located at a site having a Seismic Design Category D according to ASCE 7-16 [7] with a design earthquake spectral acceleration at short period, S_{DS} equal to 1.0 g. Based on the results of the eigenvalue analysis, the first three natural periods of the case study building are $T_1 = 1.30$ s, $T_2 = 0.45$ s, and $T_3 = 0.25$ s.

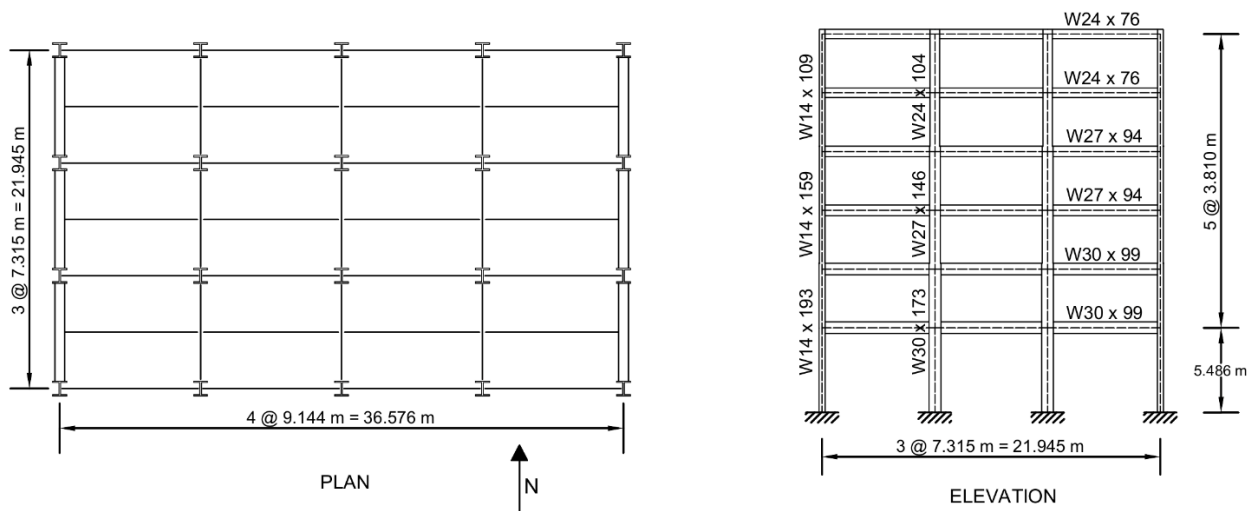


Fig. 2 – Six-storey case study steel building considered in design example.

4.2 Mechanical piping layout and properties

The mechanical piping layout selected for the design example was assumed part of the water supply piping system suspended from the top floor of the case-study building described in the previous section. Figure 3 shows a plan view of the horizontal piping layout selected. The system includes three separate pipelines: 1) a cold-water distribution line, 2) a hot-water distribution line, and 3) a hot-water recirculation line. The system includes one 17-m long main feed line connected to a perpendicular 35-m long cross main line. For simplicity,



the effects of the vertical risers and outlets that would connect to the three horizontal pipelines in a real system are neglected. All pipes in the system are assumed to be made of black standard steel not in accordance with ASME B31 [22] with a diameter of 127 mm (5 inch) along with a wall thickness of 6.5 mm. All pipe elbows and longitudinal splices are assumed threaded connections. The unit weight of each water filled pipe, w_p , is equal to 0.31 kN/m.

4.3 Seismic restraint configurations and properties

The pipes are supported by unbraced trapezes used to support vertical gravity loads only (static supports) and sway braced trapezes providing transverse or longitudinal supports. The positions of the vertical static supports are indicated in Fig. 3 and are based on a standard static design considering the self-weight of the water filled pipelines.

General views and key dimensions of the transverse and longitudinal sway braced trapezes are shown in Fig. 4a and 4b, respectively. For both directions, the vertical supports are provided by a horizontal channel and two vertical steel channels (all 41 mm deep) connected to the top floor slab by rail supports. The vertical channels are connected to the horizontal channel by pipe ring saddles. Each of the three pipes is restrained inside a pipe ring that is connected to the horizontal channel by a short (50 mm long) vertical 10-mm diameter threaded rod. The transverse and longitudinal seismic restraints are provided by one and two diagonal channels, respectively. Each diagonal channel is oriented at 45° with respect to the vertical and is connected to the ends of the horizontal channel and to the ceiling slab by channel hinges. The unbraced trapezes are identical to that shown in Fig. 4 but with the diagonal channels omitted.

The design properties for the sway braced trapezes used in this design example are based on the quasi-static cyclic testing conducted by Perrone *et al.* [23] on standard configurations of braced trapezes. Table 1 lists the mean values of the peak strength ($F_{max,p}$), the yield displacement ($\Delta_{y,p}$) and the ultimate displacement ($\Delta_{u,p}$) extracted from these test results and used for the design of the two sway braced trapeze configurations.

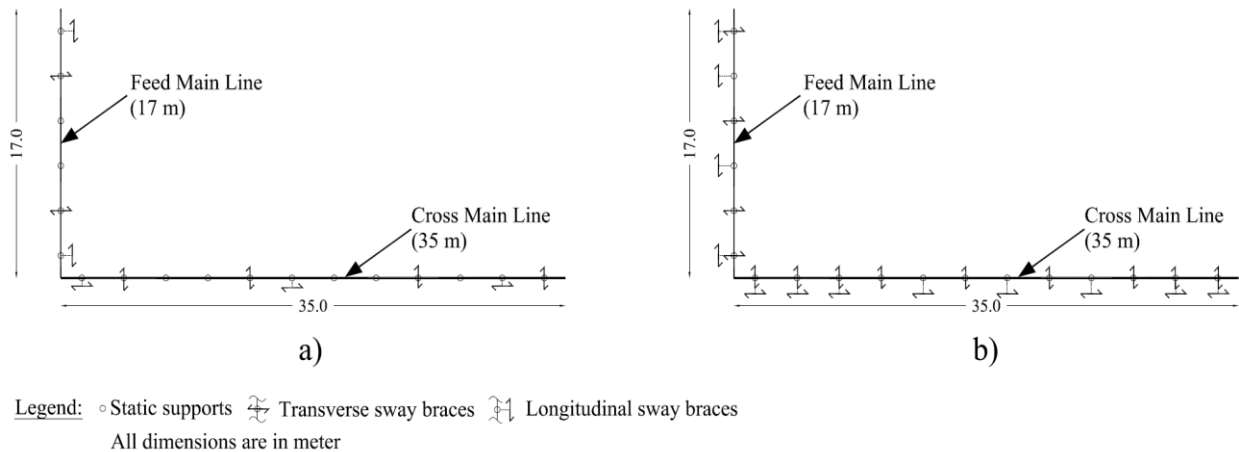


Fig. 3 – Plan view of mechanical piping layout selected for design example with sway braces, a) ASCE 7-16 force-based design (for $R_p=4.5$) and b) Direct Displacement-Based Design.

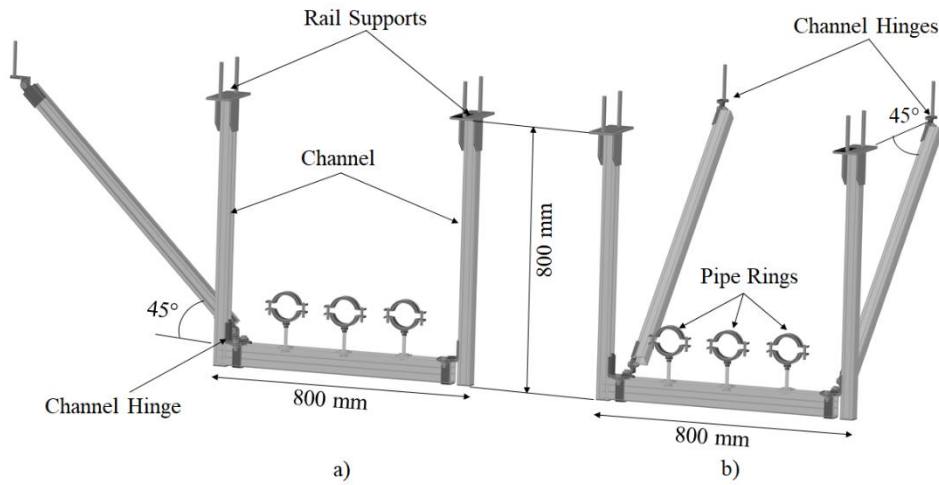


Fig. 4 – a) Transverse and b) Longitudinal sway braced trapezes.

Table 1 – Properties of sway braced trapeze systems based on test results by Perrone *et al.* [24].

Direction	Mean Properties		
	$F_{\max,p}$ (kN)	$\Delta_{y,p}$ (mm)	$\Delta_{u,p}$ (mm)
Transverse	7.88	13.1	24.9
Longitudinal	11.0	17.3	53.5

4.4 ASCE 7-16 force-based seismic design

First, the force-based procedure included in ASCE 7-16 [7] was applied to perform the seismic design of the transverse and longitudinal sway braced trapezes. The design is based on insuring that the horizontal equivalent static design force, F_{ph} , given by Eq. (1) is less or equal than the characteristic strength of the sway braced trapeze, F_{Rk} multiplied by a resistance factor, ϕ . For simplicity in this design example, F_{Rk} is taken as the mean strength from the Perrone *et al.* [23] tests ($F_{Rk} = F_{\max,p}$ from Table 1) and ϕ is taken equal to 0.8. No vertical seismic effect is considered for the seismic design of sway braced trapezes [7].

With $\phi F_{Rk} \geq F_{ph}$ and representing in Eq. (1) the operating weight of the piping, W_p , as the product of the unit weight of the total number of water filled pipe, N_p , (multiplied by a factor of 1.15 to take into account the weight of the fittings and welded connections) by the spacing of the sway braces, s_p , i.e. $W_p = 1.15N_p w_p s_p$, the required spacing of the sway braced trapezes, s_p , can be obtained as follows:

$$s_p \leq \frac{\phi F_{Rk} R_p}{0.4 a_p S_{DS} I_p} \frac{1}{1.15 N_p w_p} \frac{1}{\left(1 + 2 \frac{z}{h}\right)} \quad (6)$$

where $a_p = 2.5$ and $R_p = 4.5$ per ASCE 7-16 [7] requirements for steel piping not in accordance with ASME B31 [22] standard with threaded joints, $I_p = 1$ for non-critical non-structural elements and $z/H = 1$ for the piping system suspended from the top floor of the case-study building. Substituting the numerical values of the other parameters defined before in Eq. (6) yields required spacing of the sway braces, s_p , equal to 12.4 m in the longitudinal direction and 8.8 m in the transverse direction of the piping. Figure 4a shows the resulting layouts of transverse and longitudinal sway braced trapezes to be installed in the feed and cross main lines that meet these spacing values and satisfy the ASCE 7-16 [7] force-based design formulation.



4.5 Direct displacement-based seismic design

In this section, the steps described in Section 3 are applied to design the transverse and longitudinal sway braced trapezes according to the proposed DDBD procedure. The design was performed for two different performance objectives linked to different values of the design spectral acceleration at short period: $S_{DS} = 0.5$ g and $S_{DS} = 1.0$ g. The first performance objective is associated with damage prevention in the sway braced trapezes under frequent earthquakes represented herein by half the design earthquake intensity ($S_{DS} = 0.5$ g). This first damage prevention performance objective is assumed to be met at a target displacement equal to the yield displacement, $\Delta_{y,p}$ of the sway braced trapezes. Perrone *et al.* [23] observed that at this level of displacement there was no significant damage to the tested sway braced trapezes. This performance objective is associated with target displacements of 13.1 and 17.3 mm for the longitudinal and transverse sway braced trapezes, respectively (Table 1). The second performance objective is associated with life-safety prevention under design earthquakes ($S_{DS} = 1.0$ g). This life-safety prevention performance objective is associated with collapse prevention of the sway braced trapezes and is assumed to be associated with an ultimate displacement causing a 20% strength loss, $\Delta_{u,p}$, of the sway braced trapezes. Based on the test results by Perrone *et al.* [23] listed in Table 1, the target displacements $\Delta_{t,p}$ are $\Delta_{u,p} = 24.9$ mm and 53.5 mm for the transverse and longitudinal sway braced trapezes, respectively. The required spacing between sway braced trapezes, s_p , can be obtained by insuring again that the seismic demand expressed by Eq. (5) is less than the factored resistance of each sway braced trapeze:

$$s_p \leq \frac{gT_{eq,p}^2}{4\pi^2\Delta_{t,p}} \frac{\phi F_{R,k}}{1.15N_p w_p} \quad (7)$$

where all the variables were previously defined. Details of the derivation of Eq. (7) is provided by Filiatrault *et al.* [9]. Based on the experimental results obtained by Perrone *et al.* [23], Merino *et al.* [24] developed simple damping models for both transverse and longitudinal channel sway-braced trapezes. The resulting $\xi_{eq,p} - \Delta_{t,p}$ relationships can be expressed as follows:

$$\xi_{eq,p} = \frac{0.65}{\pi} \left(1 - \frac{0.76}{\Delta_{t,p}} \right) \geq 0 \text{ for transverse sway braced trapezes} \quad (8)$$

$$\xi_{eq,p} = \frac{0.59}{\pi} \left(1 - \frac{1.42}{\Delta_{t,p}} \right) \geq 0 \text{ for longitudinal sway braced trapezes} \quad (9)$$

where $\Delta_{t,p}$ is in mm.

To construct the top floor design relative displacement response spectrum, S_{DF} , for the case-study building, the methodology proposed by Merino *et al.* [19] was adopted. Figure 5 shows the resulting design top floor relative displacement response spectra for the case-study building. For the transverse sway braced trapezes, the floor response spectra are plotted for an equivalent viscous damping ratio of 20% for the target displacements associated with both seismic intensity levels ($S_{DS} = 0.5$ g and $S_{DS} = 1.0$ g) according to Eq. (8). For the longitudinal sway brace trapezes, the floor response spectra are plotted for 17% and 18% of critical according to Eq. (9) for the target displacements associated with $S_{DS} = 0.5$ g and $S_{DS} = 1.0$ g, respectively.

These top floor design relative displacement response spectra were used to complete the seismic design of the sway braced trapezes according to the DDBD procedure described in Section 3. Table 2 summarizes the resulting required spacing between adjacent sway braced trapezes, s_p , for the two performance objectives considered.

Table 2 – Required spacing between adjacent sway braced trapezes per the proposed DDBD methodology.

	$S_{DS} = 0.5$ g	$S_{DS} = 1.0$ g
s_p for transverse sway brace trapezes	7.04 m	4.27 m
s_p for longitudinal sway brace trapezes	9.96 m	4.65 m

The resulting spacing of the sway braced trapezes from the DDBD procedure for both the transverse and longitudinal directions is governed by the life-safety prevention performance objective ($S_{DS} = 1.0$ g). Figure



4b shows the resulting layouts of transverse and longitudinal sway braced trapezes to be installed in the feed and cross main lines that meet these spacing values and satisfying the proposed DDBD formulation.

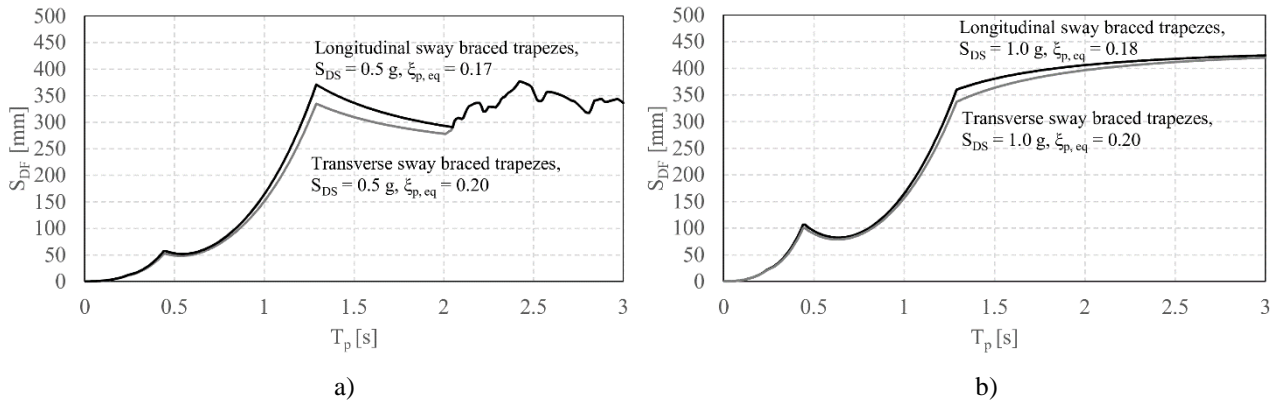


Fig. 5 – Top floor design relative displacement response spectra, after [19]; a) design spectra with $S_{DS} = 0.5g$, b) design spectra with $S_{DS} = 1.0g$.

5. Design Example Appraisal

In this section, the seismic performance of the mechanical piping systems designed according to the force-based and DDBD approaches are assessed and compared in terms of maximum displacements of the sway braced trapezes. A cascading approach was followed by performing nonlinear time history (NLTH) analyses. For this purpose, the case-study steel frame was analysed with an ensemble of 44 ground motions to generate the floor input motions, these floor motions were then used to analyse the mechanical piping system and to evaluate the maximum displacements in the transverse and longitudinal sway braced trapezes. The analyses were performed only for the design intensity level ($S_{DS} = 1.0g$) that controlled the DDBD design.

5.1 Selection and scaling of earthquake ground motions

The nonlinear dynamic response analyses of the case-study frame shown in Fig. 2 were conducted using the FEMA P695 far-field ground motion set [25] composed of 22 pairs (44 records in total) of horizontal ground motions. The ground motions were scaled in terms of the median spectral acceleration at the fundamental period of the case-study frame ($T_1 = 1.30s$) based on the ASCE 7-16 design ground acceleration spectrum [7] for the assumed site. This design ground spectrum is anchored by a design spectra acceleration at short period $S_{DS} = 1.0g$ and at a 1-second design spectral acceleration $S_{D1} = 0.6g$.

5.2 Numerical modelling

The numerical models of the case-study frame and of the piping system were developed using the OpenSees software [26] using a cascading approach. The interaction between the structural and non-structural elements was neglected in this cascading approach considering the small weight of the piping system compared to the weight of the supporting structure.

The model of the case-study steel frame was developed, in OpenSees. Fibre sections were assigned to locations where plastic hinges were expected to occur (i.e. ends of all the beams and columns). The fibre sections of the W shape steel sections were discretized using 20 fibres along the depth and one fibre along the thickness of the web, and six fibres along the thickness and one fibre along the width of each of the flanges. The steel properties were simulated in OpenSees using the Steel02 material assuming a 2.0% hardening ratio. The sections were assumed to have a curvature ductility capacity of 11. Therefore, loss of strength was modelled using the MinMax material model in OpenSees assuming that the material loses all its strength once a strain of 11 times the yield strain of the A36 steel is reached. The effects of the concrete slab were captured by assigning a rigid diaphragm constraint to all the nodes of each floor. The second order effects caused by the inner frames of the building were modelled using a P-delta leaning column. Committed stiffness Rayleigh



damping at the first and third modes of the structure was assigned to the model with a 2% damping ratio. The time step for the NLTH analyses was taken as 0.001s for all the ground motions. Note that five of the ground motions presented in Section 6.1 caused the building to collapse (i.e. collapse rate of 5/44 or 11.4%) under the ground design spectrum with $S_{DS} = 1.0$ g. These five collapsing ground motions were not considered in the assessment of the force-based and DDBD non-structural design procedures. None of the ground motions records caused the building to collapse for the seismic intensity with $S_{DS} = 0.5$ g.

Numerical models of the different mechanical piping system designs were also developed in OpenSees. All pipes were modelled as elastic frame elements in the same horizontal plane located at a drop height of 800 mm from the top slab of the case study building (see Fig. 4). All nodes were free to deform in translations and rotations except at the locations of vertical gravity load trapezes (static supports), where the vertical translations were constrained. The longitudinal and transverse sway braced trapezes were modelled by horizontal non-linear springs in their bracing directions using the Pinching4 uniaxial material model available in OpenSees. The hysteretic properties of each Pinching4 hysteretic spring were obtained by fitting the global force-displacement relationship obtained from the quasi-static cyclic testing conducted by Perrone *et al.* [23].

The mechanical piping system was analysed under two-dimensional horizontal top floor motions. Vertical floor excitation was neglected in this study. For each seismic intensity, the (non collapsing) horizontal floor motion components obtained on the top floor of the case-study building were combined to create horizontal floor motions pairs. Since the mechanical piping system is a spatial structure that can be oriented in any of the two principal directions of the supporting case study building, the horizontal components were then rotated 90° from each other to double the horizontal floor acceleration pairs.

5.3 Numerical results

The results of the NLTH analyses are assessed in terms of empirical cumulative distribution functions (CDFs) of peak transverse and longitudinal displacements in the sway braced trapezes for the two design alternatives (ASCE 7-16 force-based design and DDBD alternative) under the controlling design ground motions ($S_{DS} = 1.0$ g), as shown in Fig. 6. The target displacement associated with the life-safety prevention performance objective is indicated by a vertical dashed line in each plot.

The results shown in Fig. 6 indicate that the sway braced trapezes designed according to the ASCE 7-16 force-based design procedure fail to meet the target displacements in both directions. The median (CDF = 0.5) peak displacements obtained with this design procedure exceed the target displacements by 45 mm (2.8 times) and 14 mm (1.3 times) in the transverse and longitudinal directions of the sway braced trapezes, respectively. The resulting empirical probabilities of exceedance of the target displacements are approximately equal to 74% (CDF = 0.26) and 67% (CDF = 0.33) for the transverse and longitudinal sway braced trapezes, respectively.

The sway braced trapezes designed according to the proposed DDBD procedure meet the target displacements in both directions. The resulting lognormal probability of exceedance of the target displacement is essentially 0% in both directions.

These results demonstrate the effectiveness of the DDBD procedure. At the same time, the DDBD yields conservative designs due mainly to the three-dimensional response of the piping systems. The longitudinal sway braced trapezes installed in the feed main line offer also bracing in the transverse direction of the cross main line and vice and versa. The level of conservatism could be reduced by increasing the resistance factor, ϕ , on the characteristic strength of the sway braced trapeze in Eq. (7), or by considering the contribution of sway braced trapezes in adjacent main lines perpendicular to each other.

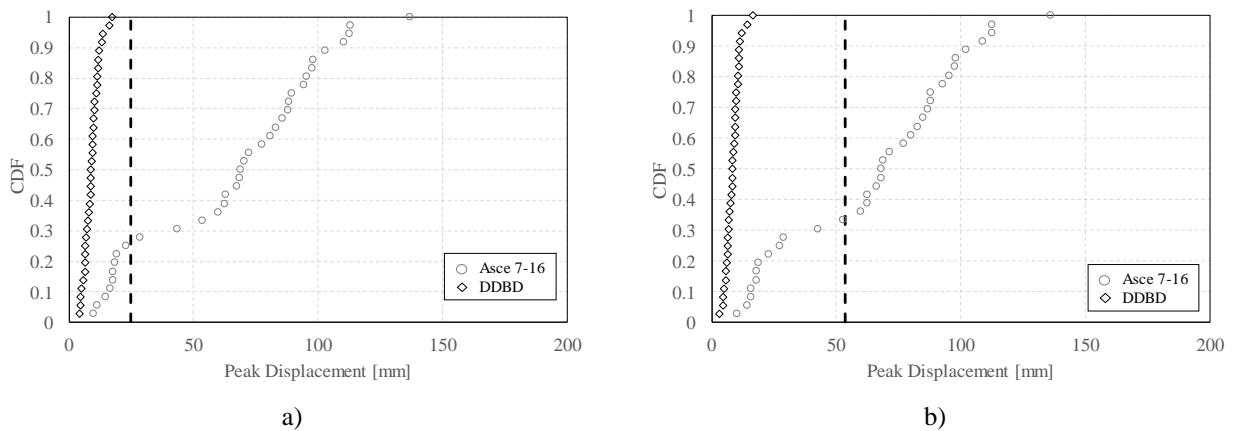


Fig. 6 – Cumulative Distribution Functions (CDFs) for Peak Displacements in Sway Braced Trapezes for ASCE 7-16 Design and DDBD, $S_{DS} = 1.0$ g, a) Transverse direction and b) Longitudinal direction.

6. Conclusions

This paper described the development and application of a direct displacement-based seismic design to non-structural building elements. The proposed design procedure applies mainly to acceleration-sensitive non-structural elements suspended or anchored at a single location (floor) in the supporting structure and for which damage is the result of excessive displacements (e.g. piping systems, cable trays, suspended ceilings, etc.). A numerical example of the direct displacement-based seismic design of a horizontal mechanical piping system suspended from the top floor of a case-study six-storey steel building assumed to be located in a high seismicity site in the west coast of the United States was presented and compared with the force-based design procedure of ASCE 7-16. Both design alternatives were evaluated through non-linear time-history dynamic analyses. The results showed that the proposed direct displacement-based seismic design procedure satisfied well the performance objectives, while the ASCE 7-16 did not.

7. Acknowledgements

The work presented in this paper was conducted within the framework of the project “Dipartimenti di Eccellenza”, funded by the Italian Ministry of Education, University and Research at IUSS Pavia. The EUCENTRE Foundation is gratefully acknowledged for provided financial support to the first author of this paper. The authors gratefully acknowledge also the Italian Department of Civil Protection (DPC) for their financial contributions to this study through the ReLUIS 2019-2021 Project.

8. References

- [1] Perrone D, Calvi PM, Nascimbene R, Fischer E, Magliulo, G. (2018): Seismic performance and damage observation of non-structural elements during the 2016 Central Italy Earthquake. *Bulletin of Earthquake Engineering*, DOI: 10.1007/s10518-018-0361-5.
- [2] Ercolino M, Petrone C, Coppola O, Magliulo G (2012): *Report sui danni registrati a San Felice sul Panaro (Mo) in seguito agli eventi sismici del 20 e 29 maggio 2012 – v1.0*. available on line: <http://www.reluis.it>.
- [3] Filiatrault A, Uang CM, Folz B, Christopoulos C, Gatto K (2001): Reconnaissance report of the February 28, 2001 Nisqually (Seattle-Olympia) earthquake. *Structural Systems Research Project Report No. SSRP-2000/15*, Department of Structural Engineering, University of California, San Diego, La Jolla, CA, 62 pp.
- [4] NIST GCR 18-917-43 (2018): *Recommendations for improved seismic performance of nonstructural elements*. Applied Technology Council, CA.
- [5] FEMA (2012): *Reducing the risks of nonstructural earthquake damage – a practical guide*. FEMA E-74, Federal Emergency Management Agency, Washington, DC, USA.



- [6] CEN (2004): *EN-1998-1:2004: E: Eurocode 8 – Design provisions for earthquake resistant structures*. Comité Européen de Normalization, Brussels, Belgium.
- [7] ASCE (2016): *ASCE 7-16: Minimum design loads for buildings and other structures*. American Society of Civil Engineers, Reston, Virginia, USA, 889 p.
- [8] Filiatrault A, Perrone D, Merino RJ, Calvi GM (2018): Performance-based seismic design of non-structural building elements. *Journal of Earthquake Engineering*, DOI: 10.1080/13632469.2018.1512910.
- [9] Singh MP, Moreschi LM, Suárez LE, Matheu EE (2006a): Seismic design forces. I: rigid nonstructural components. *Journal of Structural Engineering*, American Society of Civil Engineering, **132**(10), 1524–1532.
- [10] Singh MP, Moreschi LM, Suárez LE, Matheu EE (2006b): Seismic design forces. II: flexible nonstructural components. *Journal of Structural Engineering*, American Society of Civil Engineering, **132**(10), 1533–1542.
- [11] Kehoe B, Hachem M (2003): Procedures for estimating floor accelerations. *Seminar on Seismic Design, Performance, and Retrofit of Nonstructural Components in Critical Facilities*, ATC 29–2, Newport Beach, CA, 361–374.
- [12] Miranda E, Taghavi, S (2003): Estimation of seismic demands on acceleration-sensitive non-structural components in critical Facilities. *Seminar on Seismic Design, Performance, and Retrofit of Non-structural Components in Critical Facilities*, ATC 29–2, Newport Beach, California, 347–360.
- [13] Drake RM, Bachman RE (1996): 1994 NEHRP Provisions for non-structural components. *Journal of Architectural Engineering*, American Society of Civil Engineers, **2**(1): 26–31.
- [14] Priestley MJN, Calvi GM, Kowalsky, MJ (2007): *Displacement-based seismic design of structures*, IUSS Press, Istituto Universitario di Studi Superiori di Pavia, Pavia, Italy, 721 pp.
- [15] Sullivan TJ, Calvi PM Nascimbene R (2013): Towards improved floor spectra estimates for seismic design. *Earthquakes and Structures*, **4**(1), 109-132.
- [16] Calvi PM, Sullivan TJ (2014): Estimating floor spectra in multiple degree of freedom systems *Earthquakes and Structures, and International Journal*, **7**(1), 17-38.
- [17] Calvi PM (2014): Relative displacement floor spectra for seismic design of nonstructural elements. *Journal of Earthquake Engineering*, **18**(7), 1037-1059.
- [18] Vukobratović V, Fajfar P (2017): Code-oriented floor acceleration spectra for building structures. *Bulletin of Earthquake Engineering*, **15**, 3013-3026.
- [19] Merino R, Perrone D, Filiatrault A (2019): Consistent floor response spectra for performance-based seismic design of non-structural elements. *Earthquake Engineering & Structural Dynamics*, DOI: <https://doi.org/10.1002/eqe.3236>.
- [20] Filiatrault A, Tremblay R, Christopoulos C, Folz B, Pettinga D (2013) *Elements of earthquake engineering and structural dynamics - third Edition*, Polytechnic International Press, Montreal, Canada, 874 pp.
- [21] Jacobsen LS (1930): Steady forced vibrations as influenced by damping. *ASME Transactions*, American Society of Mechanical Engineers, **52**(1), 169-181.
- [22] ASME B31(2018): *Standards of pressure piping*. American Society of Mechanical Engineers, New York, NY, USA.
- [23] Perrone D, Filiatrault A, Peloso S, Brunesi E, Beiter C, Piccinin R (2019): Experimental seismic performance evaluation of suspended piping restraint installations, *Bulletin of Earthquake Engineering*, DOI: <https://doi.org/10.1007/s10518-019-00755-5>.
- [24] Merino R, Perrone D, Filiatrault A (2020): Equivalent viscous damping for non-structural building elements. *17th World Conference in Earthquake Engineering*, Sendai, Japan.
- [25] FEMA (2009): *Quantification of building seismic performance factors*. FEMA P695, Federal Emergency Management Agency, Washington, D.C., USA, 421 p.
- [26] Mazzoni S, McKenna F, Scott MH, Fenves GL (2006): *OpenSees Command language manual*. Pacific Earthquake Engineering Research Center, Berkeley, California.